JOURNAL OF MATERIALS SCIENCE 17 (1982) 2141–2153

Long-term growth of superalloy γ' particles

P. K. FOOTNER, B. P. RICHARDS
GEC Hirst Research Centre, Wembley, Middlesex, UK

The microstructures of five commercially available nickel-based superalloys (NIM80A, NIM90, NIM105, IN738, IN939) have been studied after heat-treatments at 4 different temperatures and for times up to 15 000 h (170 samples). In all cases for moderate times and temperatures the mean γ' dimension increased linearly with the cube root of time with an activation energy of 250 to 272 kJ mol^{-1} K^{-1}. However, at high values of time and temperature some deviations from this behaviour were observed on two of the superalloys. These were accompanied by marked morphological changes thought to be due to re-solution effects. Extended analysis of the particle-size distributions suggests a correlation with the distribution functions predicted by the Lifschitz–Slyosov theory modified to take account of encounters between growing particles. The microstructural data so obtained have been used in failure diagnosis. Attempts have been made to explain the changes in γ' shape with respect to long-term composition.

1. Introduction

Nickel-base superalloys are widely used in applications such as gas turbines, where high strength and stability at elevated temperatures are routinely required. Over the past decade, significant advances have been made in the development of new superalloys which are capable of operating at high service temperatures, thus enabling higher engine efficiencies to be realized. All these superalloys are strengthened by the precipitation of a coherent $Ni_3(Ti, Al)$ γ'-phase in the nickel-rich face-centered cubic (fcc) γ-matrix. The strength of the alloy depends on a number of factors (including size, volume fraction and strength of the precipitate) which are predetermined by the composition and initial fabrication details, and which are optimized to give specific superalloy performances. Of particular importance when considering new superalloys and their performance is the increase in precipitate size with exposure time at temperature (coarsening rate).

If coarsening is diffusion-controlled, the average γ' particle size should increase according [1, 2] to the relationship

$$(\bar{r}^3 - \bar{r}_0^3)^{1/3} = kt^{1/3}, \quad (1)$$

where $\bar{r}$ is the average particle radius at time t, $\bar{r}_0$ is the average particle radius at $t = 0$, and k is a temperature-dependent rate constant. A number of studies of the γ' coarsening rate in nickel and nickel-base alloys have been reported [3–8] although few data are available concerning long-term (> 1000 h) exposures. Ardell [5, 6] has demonstrated that coarsening of γ' in the Ni–Al and Ni–Cr–Al systems follows a diffusion-controlled model in which the cube law is obeyed. The coarsening rate has also been shown [9] to be independent of γ' volume-fraction. Studies carried out on commercially available superalloys [3, 4, 7, 8] have shown that in all cases the cubic relationship holds, although in the majority of these cases the exposure times investigated were very short compared with the expected lifetimes of engine components.

The slope of a plot of Equation 1 is the temperature-dependent rate constant, k, which is defined [5] as

$$k = \left(\frac{2\gamma DCV^2}{\rho^2 RT}\right)^{1/3}, \quad (2)$$

where γ is the interfacial free energy of the particle–matrix interface, D is the composite coefficient of diffusion of several atom species and is given by $D = D_0 \exp(-Q/RT)$; D_0 is a frequency factor and Q is an activation energy which is dependent primarily upon the activation energy

0022–2461/82/072141–13$04.06/0

for diffusion of Al and Ti in the matrix, but is also influenced by the inter-related diffusion of Co, Cr, and Mo away from a growing γ' particle; C is the concentration of solute (γ' forming elements) in equilibrium with a particle of infinite radius; V is the molar volume of precipitate; ρ is a numerical constant dependent on the redistribution of particles sizes; R is the gas constant and T is the temperature. Rearranging Equation 2 gives

$$\ln [k^3(T/C)] = \text{Constant} - (Q/RT). \quad (3)$$

The activation energy can therefore be determined from the slope of a plot of $\ln [k^3(T/C)]$ against $(1/T)$.

The purpose of the present work has been to study the effects of long-term (up to 15 000 h) heat-treatments on the γ'-precipitates in five commercially available superalloys when heat-treated at and above the expected service temperatures. Two uses of the data thus generated were anticipated. Firstly, by analysing the growth of the γ'-particles over a wide range of times and temperatures, an information and micrograph library could be established which could be used in future failure diagnosis. Secondly, by studying these superalloys it was hoped that the data produced would be of significant value in assessing factors relevant to the design of future gas turbines.

2. Experimental procedure

In an attempt to provide the present study with as broad a base as possible, samples constituting a factorial experiment of five superalloys (for initial heat-treatments, see Table I) aged over a wide range of times and temperatures have been examined. Of these superalloys, three (the Nimonic alloys NIM80A, NIM90 and NIM105) were well established alloys about which much information is available, one (IN738) has seen moderate use, whilst the last (IN939) represents a relatively recently developed superalloy. The four ageing temperatures (750, 810, 870 and 930° C respectively) were chosen to span the range of temperatures relevant to industrial long-life gas turbines, and the ageing times of up to 15 000 h to indicate the effects associated with actual engine service operation during the first two years of engine life.

TABLE I Initial heat treatments of the 5 superalloys

Alloy	Heat treatment		Time (h)	Temperature (°C)
NIM80A	2 stage	i	8	1080
		ii	16	700
NIM90	2 stage	i	8	1080
		ii	16	700
NIM105	2 stage	i	4	1125
		ii	16	850
IN738	2 stage	i	2	1120
		ii	24	845
IN939	4 stage	i	4	1150
		ii	6	1000
		iii	24	900
		iv	16	700

The factorial experiment results in 170 samples which necessitated the development of a special technique [10] in order to provide rapidly the required size data. The method consisted of selective etching of the γ'-phase from a polished metallographic section followed by examination in a scanning electron microscope, using the "specimen current mode". This enabled ready use of computer image analysing techniques to acquire the relevant γ'-size distributions. For each sample, 3 or 4 emissive micrographs and 6 to 10 specimen current micrographs were recorded from different and randomly chosen areas, the only selection involved being the avoidance of grain boundaries and inclusions. In those instances in which the γ'-precipitates were < 75 nm in size, measurements of the sizes involved were made visually from standard emissive micrographs, independently by two or three operators. This estimation procedure was also carried out for the small precipitates within the bi-modal distribution of superalloy IN738. The possible errors involved in obtaining the size data using these techniques have been discussed in a previous publication [10].

3. Results and discussion

Of the 5 superalloys examined, four (Nimonic alloys NIM80A, NIM90 and NIM105, and IN939) exhibited uni-modal size distributions, and corresponding modal values were conveniently measured (see Fig. 1a and b). By contrast, the fifth alloy (IN738) exhibited a bi-modal size distribution at low times and temperatures which changed gradually to a uni-modal distribution at higher times and temperatures (see Fig. 1c and d). In consequence, in a large number of the histograms, either one or two modal values, as appropriate, were obtained. However, in those cases in which overlap of the two distributions was marked, some degree

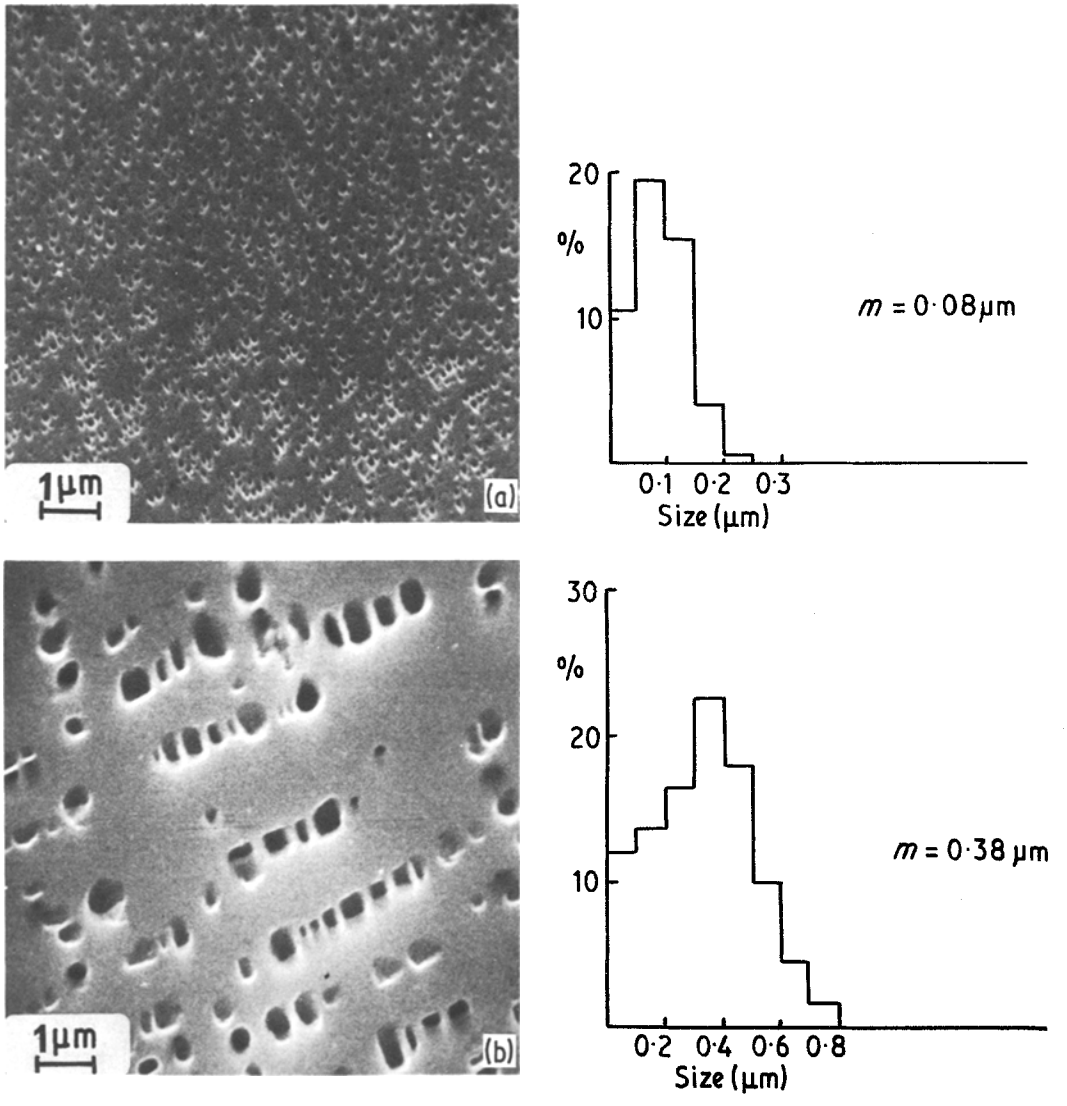

Figure 1 Typical electron micrographs and corresponding particle-size distributions for (a) NIM90 treated at 870° C for 50 h; (b) NIM90 treated at 870° C for 10 000 h; (c) IN738 treated at 750° C for 360 h and (d) IN738 treated at 930° C for 15 000 h; m is the particle size.

of separation of the distribution was undertaken based on (a) the expected shapes of the curves, and (b) the observation that the modal value of the histogram of the larger precipitates was constant over a large range of exposure times and temperatures (see below).

In view of the large number of samples (170) analysed in this work, particle-size measurements were restricted to the minimum necessary to establish acceptable accuracy in ascertaining mean and modal values. In some instances, however, particle-sizing conditions proved favourable (e.g. well defined and separated γ') for an extended analysis of the distribution function, and the measured distributions were compared with those predicted by the appropriate theories. This extended analysis was restricted to those γ'-precipitates exhibiting spherical or near-spherical shapes, for which the mathematical correction procedures are well documented. The experimental particle-size histograms were corrected from planar intercept diameters to true particle dimensions of spherical and near-spherical particles using the technique of Saltykov outlined by DeHoff [11].

Subsequently, the experimental distributions were plotted in the normal manner and compared with distribution functions predicted from the Lifschitz–Slyosov [1] and Wagner [2] theory

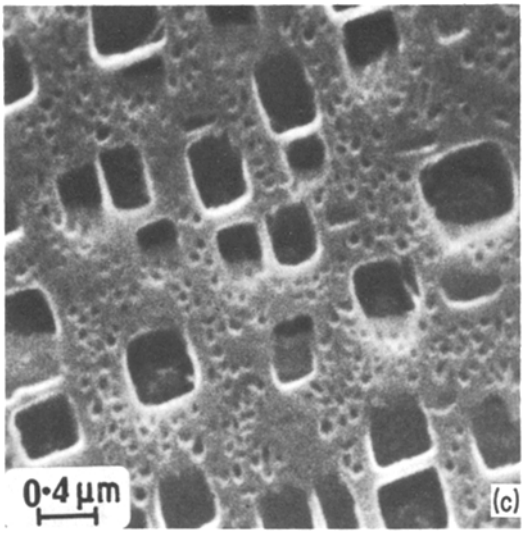

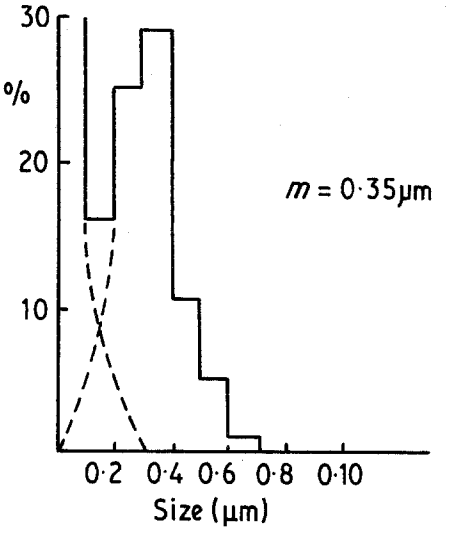

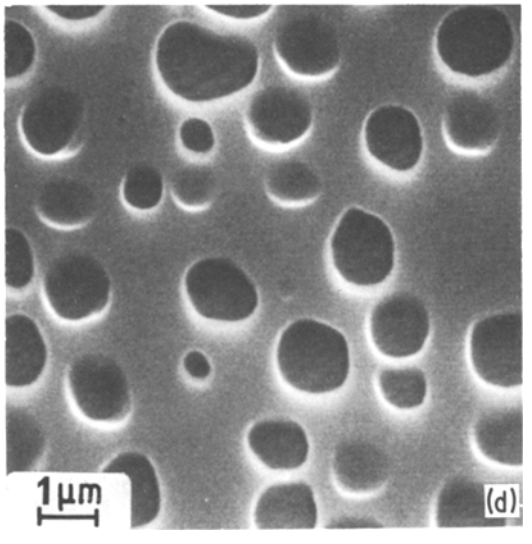

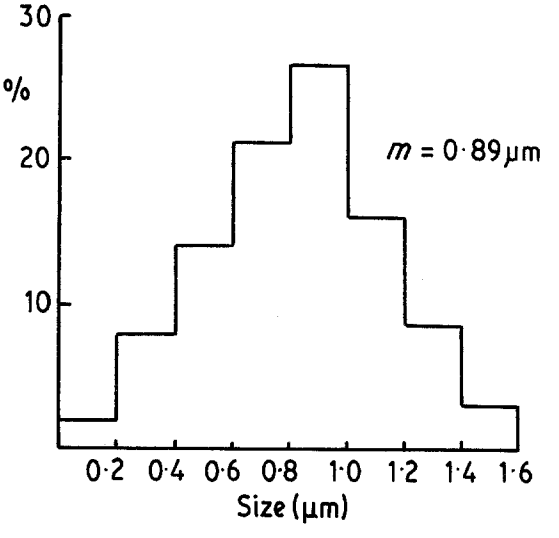

Figure 1 (Continued)

(LSW), from Ardell's modification [12] of the LSW theory (MLSW), and from the Lifschitz–Slyosov encounter-modified (LSEM) theory [13]. In the latter theory, which takes into account the spread of particle sizes resulting from adjacent precipitate encounters (i.e. coalescence), the rate of change of the mean particle size is still proportional to the cube root of the time but the rate constant is a function of volume-fraction, and so is the relative particle-size distribution. The effect of encounters is to increase the growth rate although the effect is not great; the rate constant varying by a factor of approximately three over the whole volume-fraction range [13]. It was found that in all instances of the present extended analyses, the LSEM theory gave the best fit to the experimental data. Typical examples of the experimental histograms and the LSEM distribution functions are shown in Fig. 2. The similarity between the particle-size distributions for a particular superalloy at a particular temperature indicates that the theory of a stationary distribution function holds for all times. Moreover, in the case of superalloy NIM90 at least, the particle-size distributions were similar over the range of temperatures 750 to 930° C.

This type of agreement between the experimental distribution and the LSEM distribution function was seen in all the four alloys having uni-modal distributions irrespective of exposure

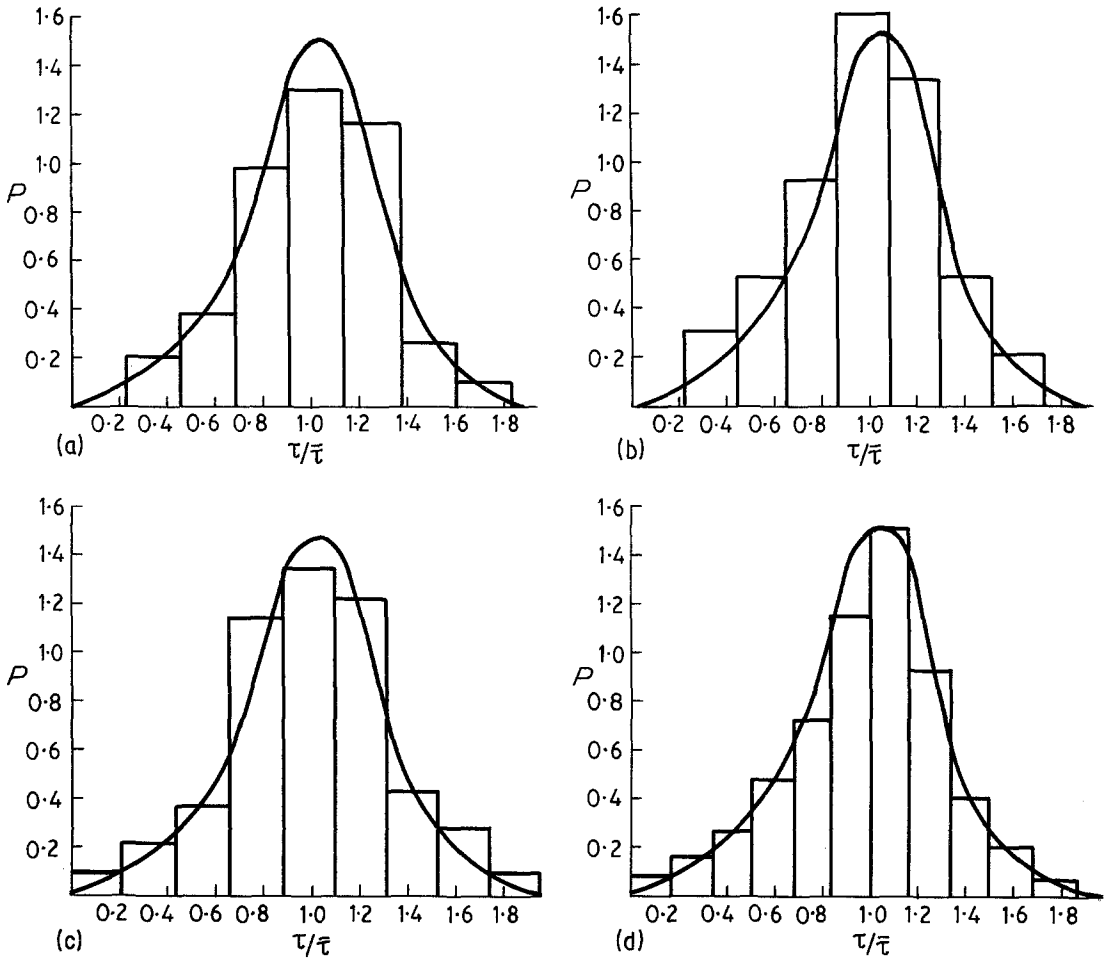

Figure 2 Comparison of LSEM distribution functions with experimental distribution of γ'-particle sizes for (a) NIM90 treated for 52 h at 930° C (22 vol% γ'); (b) NIM90 treated for 10 000 h at 810° C (24 vol% γ'); (c) IN738 treated for 15 000 h at 930° C (25 vol% γ') and (d) NIM105 treated at 10 000 h at 810° C (25 vol% γ').

time. A similar correlation was found for superalloy IN738 after long exposure times when the particle-size distribution had converted to a unimodal distribution.

In all cases of the extended analysis, when the experimental error was taken into account, the "true particle dimension" did not vary significantly from the modal value. Hence, in all further analyses or growth rates the full sets of modal values were considered.

In order to ascertain the extent to which the size data conformed to the expected relationship of the cubic root of time (see Section 1) all the modal values were plotted as function of $t^{1/3}$, see Figs 3 to 7. A careful analysis of all the emissive micrographs indicated that significant γ' shape changes occurred with exposure in all five superalloys, and these are indicated schematically as insets in Figs 3 to 7. Typical emissive micrographs illustrating these changes in superalloy IN939 are shown in Fig. 8. For Nimonic alloys NIM80A, NIM90 and NIM105 and for superalloy IN939 plots of $\ln k^3(T/C)$ against $1/T$ have been used to determine the activation energy for the coarsening process (see Section 1). In all cases the values obtained, about 250 to 272 kJ mol^{-1} K^{-1} (see Table II) were similar to those found for coarsening in other nickel-based superalloys.

3.1. Nimonic alloy 80A

In general, the growth of the γ'-phase during exposure obeys a simple $t^{1/3}$ growth law from an initial value of approximately 20 nm, the one exception being the apparent size saturation of the highest temperature samples (930° C) at a

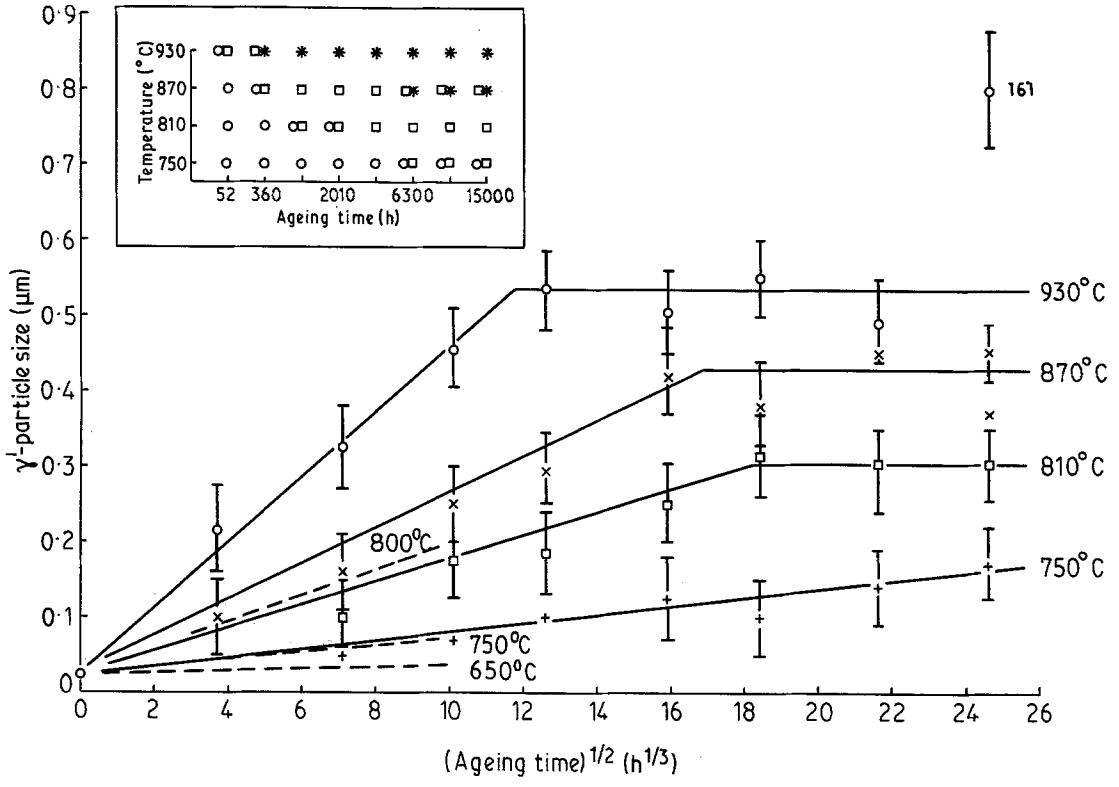

Figure 3 The variation of γ'-precipitate size with cube root of ageing time for NIM80A. The insert shows schematic changes.

value of about 0.55 μm. In addition, the data for the 870 and 810° C samples further suggest that size saturation effects may also be operative at values of approximately 0.42 and 0.32 μm, respectively. The present data are compared with published data [14] in Fig. 3 and it is evident that the general agreement over the limited ageing times available is good. During growth the γ' shape changes from the spherical to the cubic form and thence to a degenerated cubic form at the highest times and temperatures; i.e. <200 nm (spherical); ~ 200 to 400 nm (cubic); >400 nm (degenerated, irregular).

One anomaly to this general pattern of behaviour is evident in Fig. 3, i.e. Sample 161, in which the precipitate size was markedly larger than that observed in any other sample. This anomalous growth was accompanied by a considerable degeneration of shape, and is attributed to a re-solution effect, since the samples were exposed at a temperature close to the re-solution temperature of approximately 950° C. Concurrently there would have been rapid growth of any in-grain carbides which, in view of the small grain size, might have contributed to the counting statistics. The size of these carbides would in general be larger than that of the γ'-phase and hence an anomalously high value would have been recorded.

High surface energies and low coherency strains are normally associated with spherical shapes, and low surface energies and relatively high coherency strains with cubic shapes. At first sight, therefore, the initial change of shape (spherical to cubic) appears to relate to a decrease of the surface free energy. In this instance, the shape change would lower the matrix–γ' interfacial energy to $\gamma(100)$ which is known to have a very low value. Subsequently, growth selection occurs, which is favourable to those particles which are cuboidal, concurrently with alignment and the associated tendency to lower the coherency strain. However, it is likely that other factors are also operative, e.g. the equilibrium concentrations of the γ'-phase and the matrix.

The equilibrium shape is determined, therefore, by an appropriate balance between surface energy effects and strain energy, and could be a function of particle size, resulting from changes in the equilibrium matrix and γ' compositions (see below). The degeneration of the particle shape

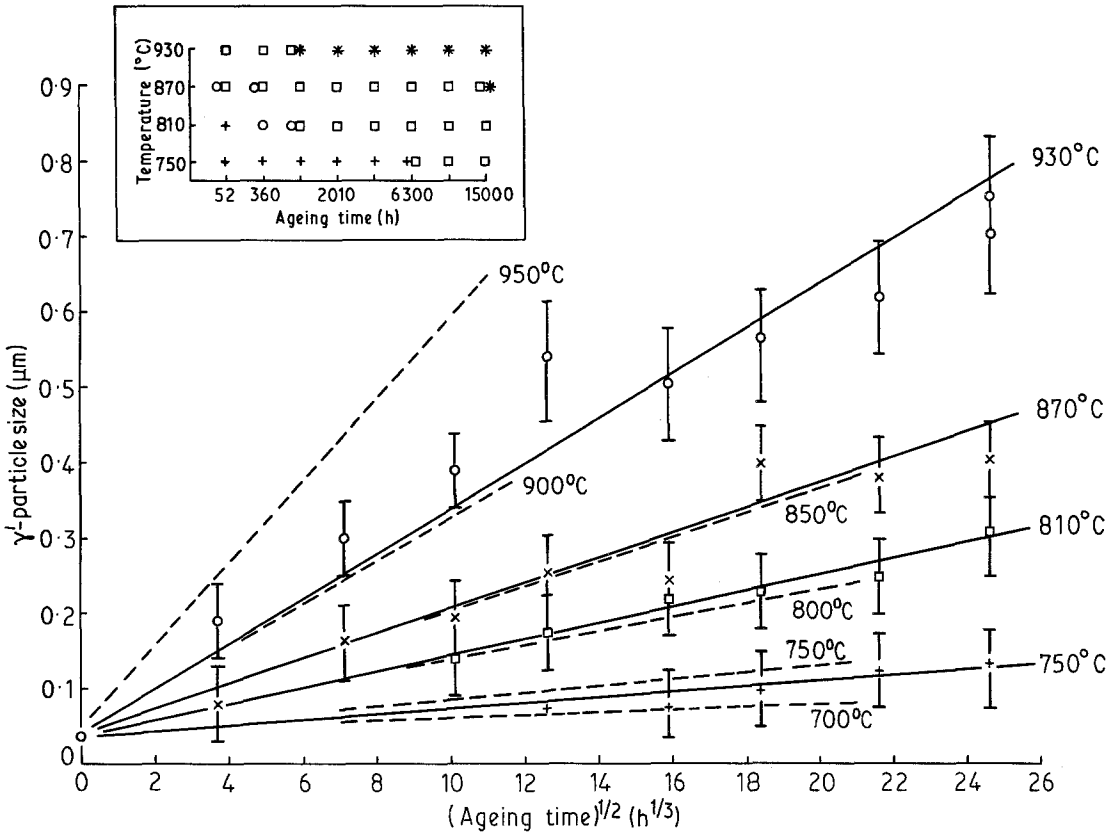

Figure 4 The variation of γ'-precipitate size with cubic root of ageing time for NIM90. The insert shows schematic changes.

for sizes >400 nm and the apparent saturation of the mean size are believed to be related to one or both of two factors, i.e., a time–temperature resolution effect, and the observed small number of particles per grain for the longest time samples.

3.2. Nimonic alloy 90

The growth of the γ'-phase again obeys the simple $t^{1/3}$ law starting from an initial value [5] of 25 nm and these findings are in excellent agreement with the limited published data, see Fig. 4. In common with NIM80A, the overall shape changes observed in this alloy can be associated with three size ranges: <150 to 200 nm (spherical); ~ 200 to 400 nm (cubic); and >400 nm (dengenerated shape).

3.3. Nimonic alloy 105

At all values of exposure time and temperature the growth of the γ'-phase (initial precipitate value of ~ 65 nm) obeys the simple $t^{1/3}$ law, see Fig. 5, but poor agreement was obtained with the published data. A two-stage heat-treatment was employed for the present samples whilst the published data are thought to relate to typical three-stage heat-treated material. The γ'-phase tends to change from the spherical to the cubic form, the critical size for the shape discrimination being ~ 200 to 250 nm.

3.4. Superalloy IN738

The variation with the cube root of exposure time of the γ' size was complex, and this is a direct consequence of the initial heat-treatments (see Table I) which had resulted in the presence of two distinct γ' populations. On ageing, the mean size of the larger population (primary particles) remained sensibly constant at a value of about 0.35 μm, whilst that of the smaller size population (secondary particles) increased, the rate of increase depending on the ageing temperature. Subsequent growth of the primary particles occurred only when the overall size distribution appeared to be uni-modal and this growth again obeyed a $t^{1/3}$ law. The maximum size attained by the secondary particles was about 0.15 to 0.17 μm, further ageing

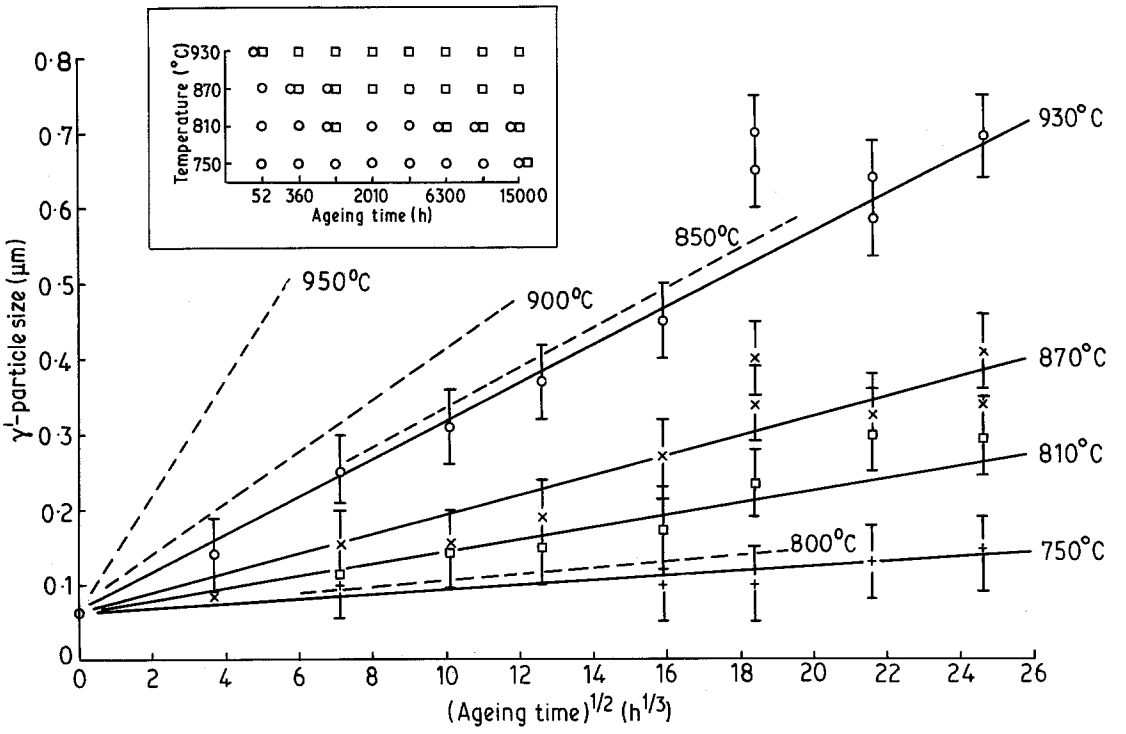

Figure 5 The variation of γ'-precipitate size with cubic root of ageing time for NIM105. The insert shows schematic changes.

resulting in their rapid disappearance, as indicated by the dotted extrapolations. The change in size of the primary phase is closely related to a change in shape (see Fig. 6). The original heat-treatments resulted in cuboidal particles (0.35 μm in size) consequent on the high degree of mismatch between the matrix and γ'-phase, but once growth of the primary particles had been initiated they transformed to roughly spherical or even "shapeless" particles.

The driving force for the growth of the primary particles is a reduction in the total mismatch strain and this process does not become operative until the secondary solute particles have attained a size and a surface concentration comparable with those of the primary particles. It appears that this condition is achieved when these particles have a mean size of approximately 0.15 to 0.17 μm. Subsequently, the now essentially single population of (primary) particles experiences normal growth kinetics. As the growth proceeds, ageing changes the matrix composition (e.g. Al and Cr etc) and hence decreases the mismatch and promotes spheroidization, as observed.

3.5. Superalloy IN939

The growth of γ' is very slow but again Equation 1 is essentially obeyed (see Fig. 7). However, some complexity is involved in that there are marked and sudden increases in the growth rates at all temperatures when the mean size was in excess of about 0.22 μm. Concurrently, there was a change in shape from spherical to cuboidal morphology. In common with NIM80A, there is an apparent size saturation of the highest temperature samples at a value of $\sim$ 0.38 μm, accompanied by a degeneration of particle shape examples of which are shown in Fig. 8. The apparently anomalously large value for the 930° C/15 000 h sample is believed to be associated with, and a direct consequence of the very small grain size of this particular sample; each grain contained only about 5 to 10 γ'-particles, with much of the γ'-phase concentrated along or near the grain boundaries. The possibility of a re-solution effect occurring in this sample was considered but rejected since the re-solution temperature for this alloy ($\sim$ 1100° C) is significantly higher than the exposure temperature of 930° C.

4. Calculation of γ–γ' interfacial energies

In a number of studies of coarsening of precipitates in Ni-based alloys it has been shown that estimates of the interfacial energy can be made by

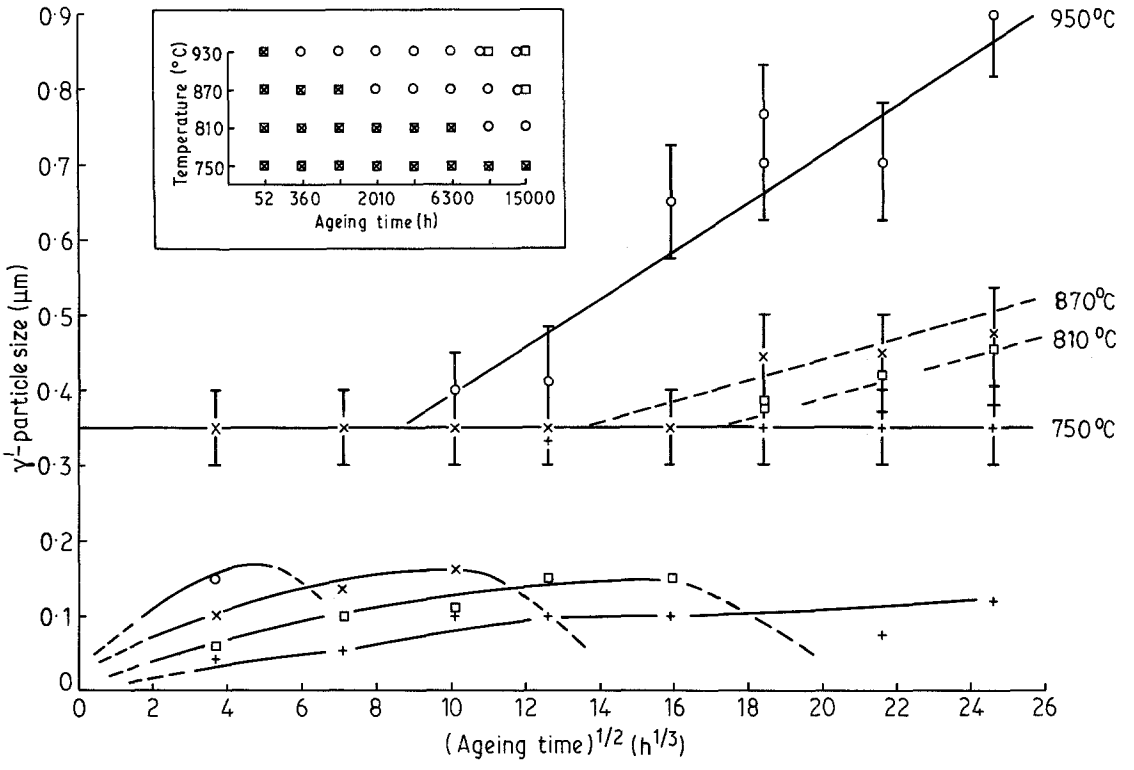

Figure 6 The variation of γ'-precipitate size with cubic root of ageing time for alloy IN738. The insert shows schematic changes.

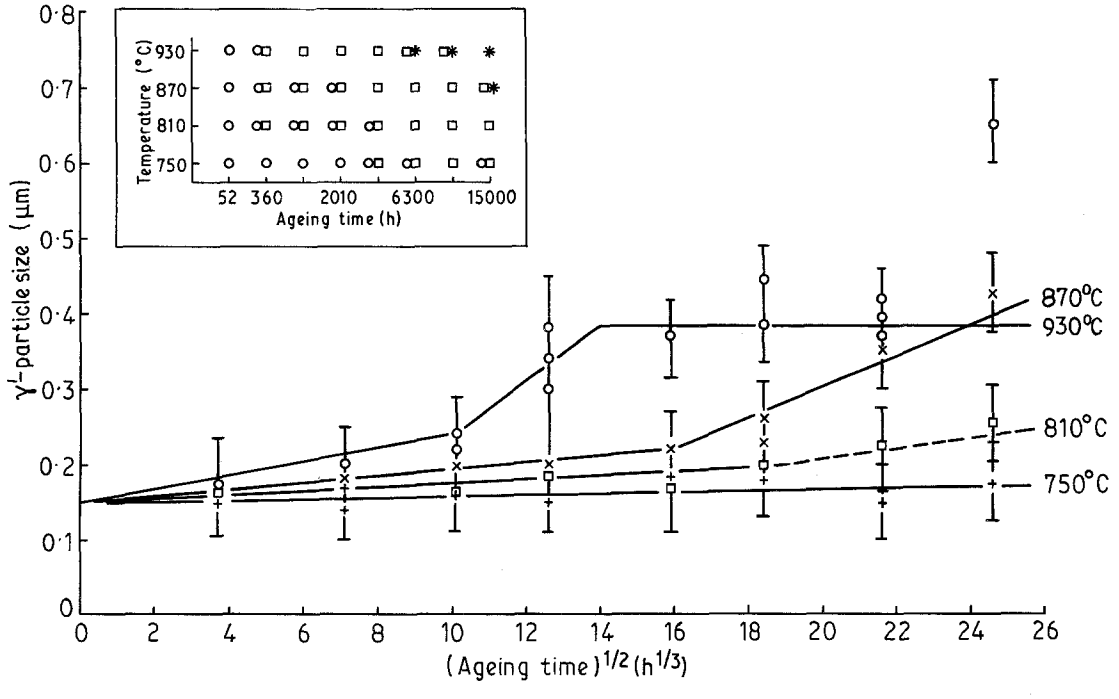

Figure 7 The variation of γ'-precipitate size with cubic root of ageing time for alloy IN939. The insert shows schematic changes.

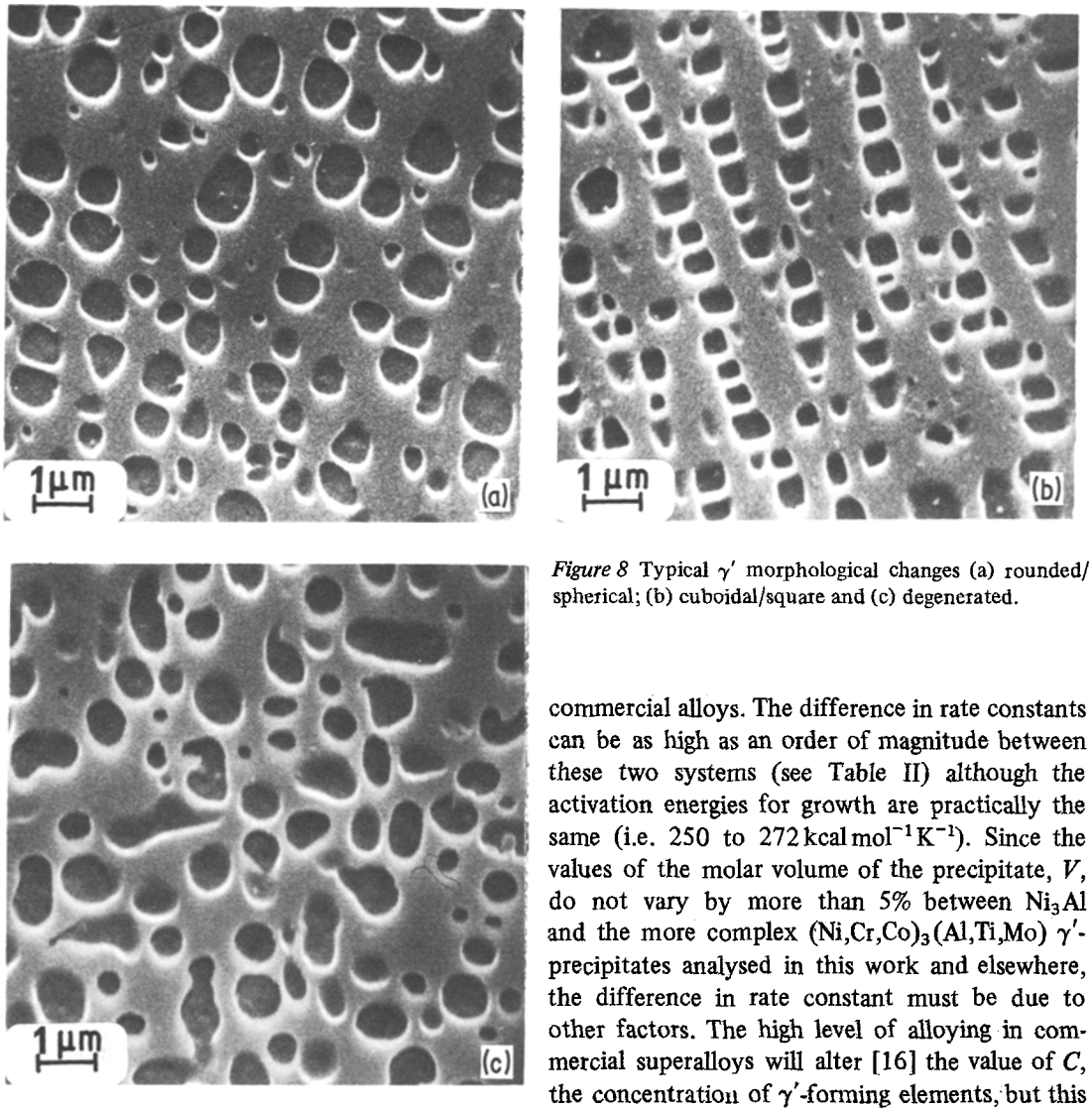

Figure 8 Typical γ' morphological changes (a) rounded/spherical; (b) cuboidal/square and (c) degenerated.

evaluating the constants and parameters in the appropriate equations, e.g. for the LSW theory. This necessitates a detailed knowledge of the solubilities and diffusion coefficients of the elements comprising the precipitate in the matrix. In the case of simple binary (i.e. Ni–Al) systems these data are readily available [15] and such calculations [5, 6] give good agreement with expected value of interfacial energies (e.g. $\gamma(100) \simeq 30\,\mathrm{erg\,cm^{-2}}$ for Ni–Al). However, in the case of commercial alloys in which matrix and precipitate contain a number of elements the solubility and diffusion data are not available.

Comparison of growth rate kinetics, as shown in Fig. 9, illustrates the marked difference between simple binary and complex multi-component commercial alloys. The difference in rate constants can be as high as an order of magnitude between these two systems (see Table II) although the activation energies for growth are practically the same (i.e. 250 to $272\,\mathrm{kcal\,mol^{-1}\,K^{-1}}$). Since the values of the molar volume of the precipitate, V, do not vary by more than 5% between Ni_3Al and the more complex $(Ni,Cr,Co)_3(Al,Ti,Mo)$ γ'-precipitates analysed in this work and elsewhere, the difference in rate constant must be due to other factors. The high level of alloying in commercial superalloys will alter [16] the value of C, the concentration of γ'-forming elements, but this variation is unlikely to account fully for this change [17]. We estimate 50% as the maximum probable variation. Hence the major source of variation must lie in the diffusion coefficients of the γ'-precipitate components (e.g. Ti, Mo, Al). These have been measured in binary systems but not in a multi-component system. The interaction between the diffusing species could effect a major variation of the diffusion coefficient. Another factor which may well be of significance is the interaction between these highly reactive elements and residual interstitial impurities, such as carbon and oxygen, in the matrix.

In view of the lack of data concerning C and D, therefore, the calculation of the interfacial energies in the present work was thought to be of doubtful significance until these data become available.

TABLE II Data for the determination of the activation energy, Q

Alloy	T (K)	k^3 ($nm^3 h^{-1}$)	C^* ($mol\,cm^{-3}$) $\times 10^{-2}$	Q ($kJ\,mol^{-1}\,K^{-1}$)
NIM80A	1023	2.3×10^2	2	274.1
	1083	4.25×10^3		
	1143	1.6×10^4		
	1203	8×10^4		
NIM90	1023	1.16×10^2	2	257.0
	1083	1.18×10^3		
	1143	6×10^3		
	1203	3.05×10^4		
NIM105	1023	1.5×10^2	2	263.7
	1083	1.2×10^3		
	1143	3.7×10^3		
	1203	1.5×10^4		
Superalloy IN939	1023	1.2×10^2	2	265.5
	1083	7.5×10^2		
	1143	1.9×10^3		
	1203	1.1×10^4		
Ni–Al [5]	898	6.13×10^1	1.77	269.5
	898	5.77×10^1	1.77	
	988	2.09×10^3	1.90	
	988	1.95×10^3	1.90	
	1023	4.60×10^3	1.96	
	1048	1.04×10^4	2.02	
Udimet 700 [16]	1144	3.8×10^3	1.06	
	1172	8.24×10^3	1.09	
	1200	2.34×10^4	1.19	
	1227	3.53×10^4	1.21	
	1255	7.41×10^4	1.30	
	1282	1.27×10^5	1.44	
	1366	6.45×10^5	1.81	

*In the present work, for the temperature range covered, C has been estimated from the limited chemical composition data available.

5. Additional investigations

In an attempt further to explain these data and fully to asses their significance, two additional investigations were undertaken.

X-ray diffraction examinations were carried out in order to ascertain the operative strain values in the matrix and in the γ'-phase by careful analysis of the shapes of the diffraction lines. In this manner it was hoped that the respective lattice parameters could be determined from the relevant peak positions, and the matrix–particle mismatch calculated. Three characteristic parameters (peak position, peak, and width at $\frac{1}{2}$peak height) were measured on freshly polished samples using an X-ray diffractometer, but it was not possible to correlate the observed variations of these parameters with exposure time or temperature. Moreover, the results obtained could be significantly influenced by the choice of experimental analysis conditions, and this variability was attributed to grain size and orientation problems. This diagnosis was confirmed using standard glancing-angle X-ray diffraction and texture camera [18] techniques. It is hoped that recourse to convergent-beam transmission electron microscopy [19] on specially thinned samples will furnish these required data.

As discussed above, the equilibrium shape of the γ'-particles is probably determined by a balance between surface energy effects and strain energy, and could be a function of particle size. It would be relevant, therefore, to know whether, and by how much, the chemical composition of the matrix is changing with exposure time and/or temperature. For example, Ardell and Nicholson [5, 6] have suggested that the concentration of the Al in the matrix changes with time, which might have a profound effect on the shape of the Ni_3Al particles. In addition, such a change might tend to decrease the matrix–particle mismatch and promote spheroidizing, and this would cer-

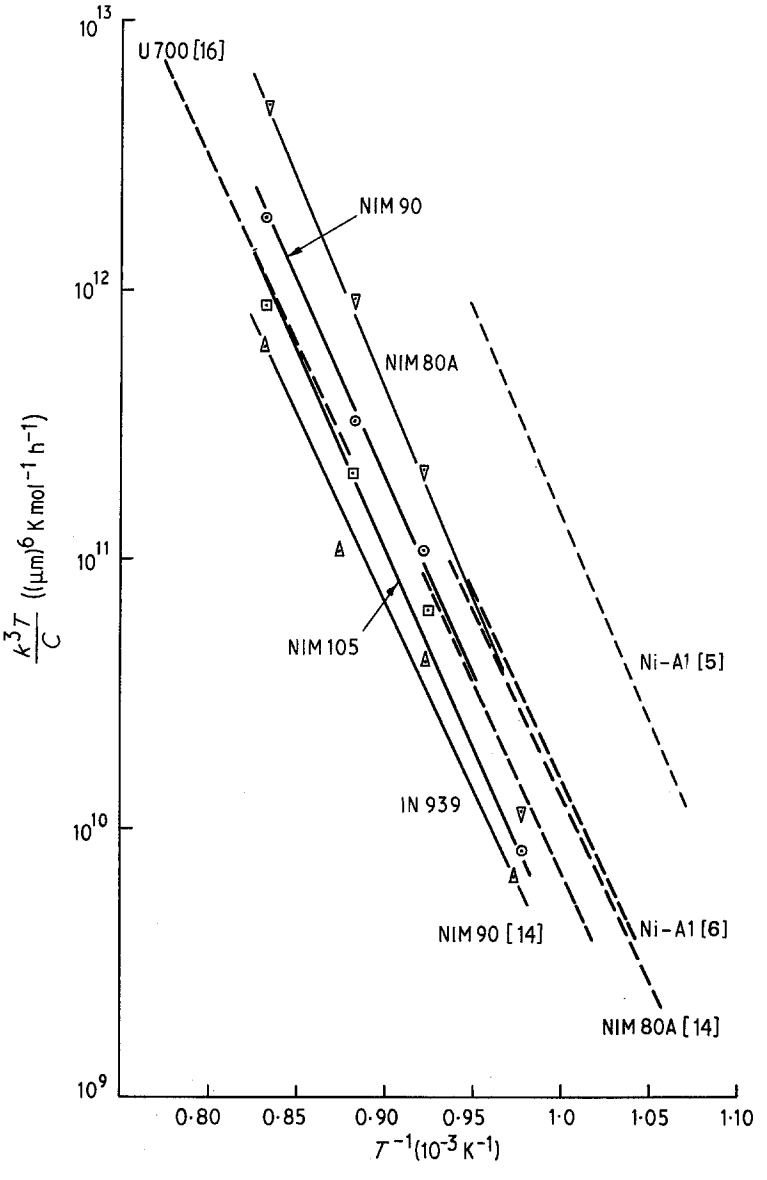

Figure 9 The variation of log $k^3(T/C)$ with $1/T$ for various Ni-based superalloys.

tainly be important in the case of superalloy IN738. The matrix concentration of other alloying elements such as chromium might also have a significant effect on these processes, in which case chemical data relating to the carbide inclusions would also be important.

In order to obtain chemical information from both the matrix and γ'-particles in a non-destructive manner (to retain the γ'-matrix geometry/strain), the sample volume must be very small, typically sub-micrometre in size. If conventional analytical methods are employed, this criterion can be accomplished only using electron-optical techniques in which the analysed volume can be limited to a micrometre or so. Recently, Betzold [20] has described a method applicable to either wavelength-dispersive or energy-dispersive analysis of X-rays (EDX) in which, it is claimed, it is possible to get the "true" chemical composition of sub-micrometre particles using an extrapolation procedure, and this has been employed in the present investigation. The results obtained suggested that the γ' composition in any one superalloy was independent of exposure time (i.e. γ' size). Moreover, the general pattern of the concentration was the same for the samples in any one alloy. A systematic analysis of the data indicated that the limits of error associated with these determinations were those to be expected from normal EDX systems (i.e. about 0.1 to 0.5% of

the sampled volume). It is probable, therefore that any subtle (but important) changes in composition would not have been monitored using this technique. Moreover, variations of composition across a γ'-particle or, more importantly perhaps, in the matrix surrounding an inclusion cannot be assessed using this procedure.

It is hoped that useful information of this kind might be obtained using an atom-probe field-ion microscope to investigate [21] the distribution of alloying elements, and investigations using this technique are in hand. The atom probe can be used [22] to analyse selectively the ordered γ' particles, the matrix and the γ'–γ interface, with a spatial resolution of < 5 nm. A recent examination [21] of IN939 superalloy has suggested that the composition of the γ'-precipitates is approximately $(Ni,Co)_3(Al,Ti,Cr)$, i.e. the Cr appears to substitute for the Al–Ti atoms in the mixed layer rather than in the Ni layer. In addition, where was some evidence to suggest that the C, Si and W levels were higher in the γ–γ' interface than in either phase. Parallel examinations using a scanning Auger microscope have been initiated.

6. Conclusions

The γ' growth in the five superalloys showed the expected $\bar{r}$ against $t^{1/3}$ linear relationship up to moderate times and temperatures of exposure. At high values of time and temperature, deviations from this relationship have been observed together with degeneration of particle morphology attributed to re-solution effects. In the case of superalloy IN939 an apparent size saturation was observed. Extended analyses suggest a correlation between the experimental particle-size distributions and the theoretical distribution functions predicted by the Lifschitz–Slyosov [1, 2] model modified by Davies *et al.* [13] to include the effect of particle encounter and coalescence. The activation energy for the coarsening process was found to be 60 to 65 kcal mol^{-1} K^{-1} which is in excellent agreement with published data for coarsening at shorter times. The causes of the changes in γ' morphology during ageing have been discussed, but lack of accurate data with regard to lattice parameters and compositions has prevented firm conclusions. The data generated in this study have been used for failure diagnosis, an example of which has been reported elsewhere [10].

Acknowledgements

The authors would like to thank Ruston Gas Turbines Limited for permission to publish this work, Mr J. Sutton for providing the samples and Mr F. W. Pearce for helpful discussions.

References

1. I. M. LIFTSHITZ and V. V. SLYOZOV, *J. Phys. Chem. Solids* **19** (1961) 35.
2. C. WAGNER, *Z. Electrochem.* **65** (1961) 581.
3. W. HOFFELNER, E. KNY, W. McCALL and R STICKLER, *Z. Werkstofftech.* **10** (1979) 84.
4. S. B. FISHER and R. J. WHITE, *Mater. Sci. Eng.* **33** (1978) 149.
5. A. J. ARDELL and R. B. NICHOLSON, *J. Phys. Chem. Solids* **27** (1966) 1793.
6. *Idem, Acta Met.* **14** (1966) 1295.
7. P. E. FLEWITT and R. A. STEVENS, *Mater. Sci. Eng.* **37** (1979) 237.
8. S. B. FISHER, K. MILLER, G. SWALLOW and R. J. WHITE, *J. Nuclear Mater.* **55** (1975) 273.
9. A. J. ARDELL and D. CHELLMAN, *ibid.* **22** (1974) 577.
10. P. K. FOOTNER and B. P. RICHARDS, *Pract. Metallogr.* **17** (1980) 489.
11. R. T. DEHOFF, *Trans. Met. Soc. AIME* **224** (1962) 474.
12. A. J. ARDELL, *Acta Met.* **20** (1972) 61.
13. C. K. L. DAVIES, P. NASH and R. N. STEVENS, *ibid.* **28** (1980) 179.
14. HENRY WIGGEN & CO, Structures of Nimonic Alloys, Publication No 3563A, January 1973.
15. R. A. SWALIN and A. MARTIN, *Trans. AIME* **206** (1956) 567.
16. E. H. VAN DER MOLEN, J. M. OBLAK and O. H. KRIEGE, *Met. Trans.* **2** (1971) 1627.
17. C. T. SIMS and W. H. HAGEL, "The Superalloys" (John Wiley & Sons, Chichester, 1972) p. 50.
18. C. A. WALLACE and R. C. C. WARD, *J. Appl. Crystallogr.* **8** (1975) 255.
19. J. A. EADES, Proceedings of EMAG 1977, edited by D. L. Misell, September 1977 Institute of Physics Conference Series No 36 (Institute of Physics, Bristol, 1977) p. 283.
20. J. BETZOLD, *Pract. Metallogr.* **14** (1977) 310.
21. P. A. BEAVEN, M. K. MILLER and G. W. D. SMITH, Proceedings of EMAG 1977, edited by D. L. Misell, September 1977 Institute of Physics Conference Series No 36 (Institute of Physics, Bristol, 1977) p. 199.
22. P. A. BEAVEN, M. K. MILLER, R. J. LEWIS and G. D. W. SMITH, Proceedings of the 23rd International Field Emission Symposium, Pennsylvania State University, 1976.

Received 30 July
and accepted 15 December 1981